RP Current Trends In Engineering And Technology (e-ISSN: 2583-5491)
Vol. 5, No. 1 (January – March 2026) pp. 19–24

RESEARCH PLATEAU PUBLISHERS

Cite this article: M.A. Rahim, H. Jeong, M.J. Ko, S. Das, Comparison of the dye-sensitized solar cell performance of two carbazole-appended unsymmetrical squaraines, *RP Cur. Tr. Eng. Tech*. **5** (2026) 19–24.

Original Research Article

Comparison of the dye-sensitized solar cell performance of two carbazole-appended unsymmetrical squaraines

Moochikkadavath Abdul Rahim[1,*], Hansol Jeong[2], Min Jae Ko[3], Suresh Das[4]

[1]Assistant Professor, Department of Chemistry, TKM College of Arts and Science, Kollam-05, Kerala, India
[2]Korea Institute of Science and Technology (KIST), South Korea
[3]Department of Chemical Engineering, College of Engineering, Hanyang University and Photo-Electronic Hybrids Research Center, National Agenda Research Division, Korea Institute of Science and Technology (KIST), South Korea
[4]Honorary Professor (Chemistry), Indian Institute of Science Education and Research, Thiruvananthapuram, Kerala, India
*Corresponding author, E-mail: abdulrahimmk@tkmcas.ac.in

ARTICLE HISTORY
Received: 02 March 2026
Revised: 26 May 2026
Accepted: 27 May 2026
Published: 12 June 2026

KEYWORDS
Dye-sensitized solar cells (DSSCs); Unsymmetrical squaraine dyes; Carbazole sensitizers; Near-infrared absorption; Photovoltaic performance.

ABSTRACT
Two carbazole-appended unsymmetrical squaraine sensitizers, SQ1 and SQ2, were designed, synthesized, and investigated for their application in dye-sensitized solar cells (DSSCs). The dyes consist of a carbazole-linked thiophene unit as the electron donor and an N-ethyl quaternized indolinium moiety bearing a cyanoacrylic acid anchoring group as the electron acceptor. The structural difference between SQ1 and SQ2 arises from the substitution pattern at the 3,6-positions of the carbazole core, where SQ1 contains bulky tert-butyl substituents while SQ2 lacks these groups. The introduction of tert-butyl groups is expected to enhance solubility in common organic solvents and reduce dye aggregation on TiO_2 surfaces, thereby improving photovoltaic performance. The target dyes were synthesized through condensation of semisquaraines with the indolinium precursor under azeotropic reflux conditions, followed by hydrolysis to obtain the final sensitizers. The synthesized dyes exhibited strong absorption in the far-red/near-infrared region, characteristic of squaraine chromophores, making them suitable candidates for DSSC applications. Comparative evaluation of the photovoltaic performance of SQ1 and SQ2 highlights the influence of carbazole substitution on the efficiency and interfacial properties of squaraine-based DSSCs.

1. Introduction

The seminal work of Grätzel and co-workers on dye-sensitized solar cells (DSSCs) marked a significant achievement towards enabling the use of sunlight as a renewable energy resource [1-5]. In DSSCs, metal-free organic sensitizers have emerged as cost-effective and environment-friendly alternatives to metal-based sensitizers [6-8]. Among the large variety of efficient metal free sensitizers, squaraine dyes are identified as promising candidates due to their high molar extinction coefficient, intense absorption in the far red/NIR region and improved photostability under ambient conditions [9-12]. Squaraine as sensitizers have attracted significant attention in view of their potential for application in a variety of fields including the development of photovoltaic devices [13-18]. Further studies on DSSCs improved the PCEs of unsymmetrical squaraine dyes considerably [19-22]. Recently, Jradi *et al.* achieved the highest PCE of 8.9% using an unsymmetrical squaraine sensitizer composed of 4,4-bis(2-ethylhexyl)-4H-silolo[3,2-b:4,5-b′]dithiophene π–bridge with cyanoacetic acid anchoring group [23].

Carbazole-based organic systems have been employed widely as active materials in various fields [24-26] and in the present work, we report the design, synthesis and characterization of two carbazole incorporated unsymmetrical squaraine sensitizers SQ1 and SQ2 (Chart 1). In both dyes, carbazole linked to thiophene unit functioned as the electron donor component whereas N-ethyl quarternized indolinium moiety with cynoacrylic acid acted as the electron acceptor component. The chemical structure of SQ1 and SQ2 differ each other only in their substitution at the 3,6 position of the carbazole moiety. The presence of bulky *tert*-butyl groups in SQ1 is expected to increase the solubility in common organic solvents and suppress the molecular aggregation on TiO_2 surfaces.

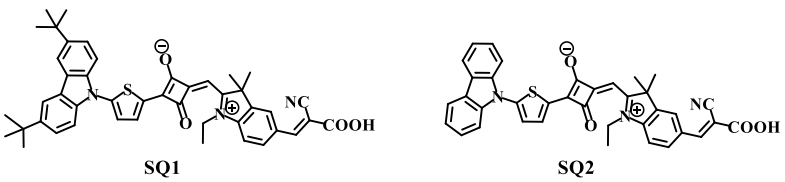

SQ1 SQ2

Chart 1: Chemical structure of target dyes.

Copyright: © 2026 by the authors. Licensee Research Plateau Publishers, India
This article is an open access article distributed under the terms and conditions of the Creative Commons Attribution (CC BY) license (https://creativecommons.org/licenses/by/4.0/).

Detailed synthesis of SQ1 and SQ2 has been shown in the Scheme 1. Condensation of semisquaraines (5 and 6) with compound 7 under azeotropic reflux conditions in n-butanol/toluene solvent mixture gave the corresponding *tert*-butyl ester squaraines and which was followed by hydrolysis using trifluoroacetic acid to get the target dyes SQ1 and SQ2 respectively. The details concerning the synthetic procedures and characterization of the dyes by ^{1}H-NMR and mass spectral analysis are described.

2. Experimental

2.1 Materials and Instruments

The precursor chemicals were purchased from Sigma-Aldrich, Spectrochem Pvt. Ltd., Alfa-Aesar, Merck and Solaronix. Synthesis of precursor units such as 5, 6 and 7 were carried out based on previous literature reports and the characterization details of the target dyes were provided in the following section [27, 28]. The ^{1}H-NMR and ^{13}C-NMR (400 and 600 MHz) were taken using Bruker Advance DPX spectrometer with trimethylsilane (TMS) as internal standard. All the mass spectra containing (M+1) peak were done by ESI technique under ThermoScientific EXACTIVE spectrometer. Absorption spectra were taken in 1.0 cm width quartz cell using Shimadzu UV-3101 PC UV-vis-NIR spectrophotometer and emission spectra were taken in 1.0 cm width quartz cell using PerkinElmer spectrofluorimeter. Electrochemical measurements were done at a scanning rate of 100 mVs^{-1}, equipped with a normal one compartment cell with Pt disk working electrode, Pt counter electrode and Ag/AgCl (sat. KCl) reference electrode. The measurements were performed in DCM solution containing 0.1 M tetrabutylammonium hexafluorophosphate (n-Bu_4NPF_6) as supporting electrolyte. The thickness of the TiO_2 film was measured by Alpha-Step IQ surface profiler (KLA-Tencor). The *Gaussian 09* software suite of quantum chemical programs was used for computational modelling and calculation at the density functional theory (DFT) level.

Scheme 1: Synthetic methodology of SQ1 and SQ2.

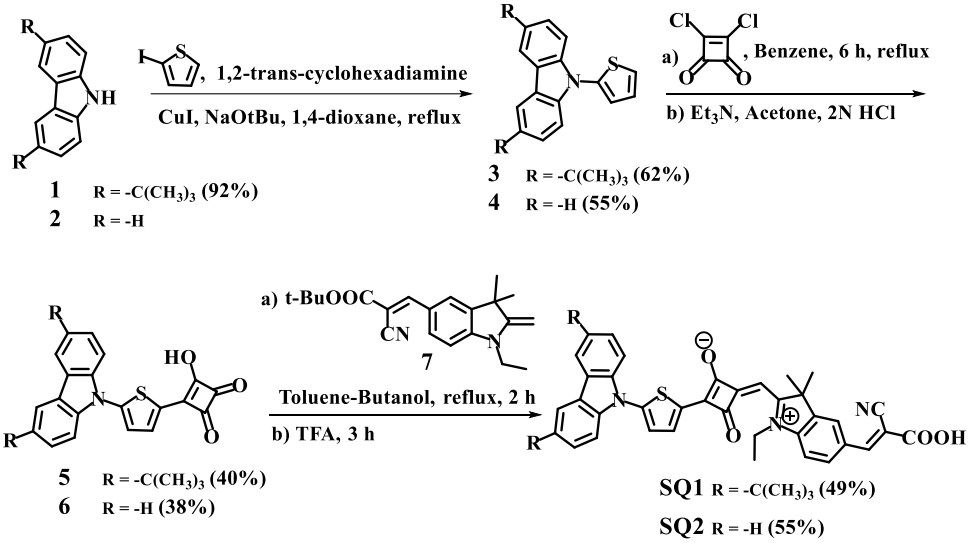

2.2 Synthesis

2.2.1 Synthesis of SQ1

130 mg (0.17 mmol) *tert*-butyl ester of unsymmetrical squaraine dye (8) was stirred with 3 mL of trifluoroacetic acid (TFA) for 3 h at room temperature. TFA was evaporated after completion of the hydrolysis which was monitored using thin layer chromatography (TLC). The crude product obtained was purified by silica gel chromatography using 10% methanol in ethyl acetate as eluent to give 60 mg of **SQ1** as blue solid (49%). ^{1}H-NMR (600 MHz, CD_3OD, TMS): δ 1.466 (s, 18H), 1.521-1.545 (t, J = 14.4 Hz, 3H), 1.887 (s, 6H), 4.493-4.515 (q, J =13.2 Hz, 2H), 6.534 (s, 1H), 7.459-7.482 (m, 1H), 7.563-7.581 (dd, J = 1.8 Hz, 10.8 Hz, 2H), 7.663-7.678 (d, J = 9 Hz, 2H), 7.719-7.733 (m, 1H), 7.995-8.001 (d, J = 3.6 Hz, 1H), 8.086-8.099 (d, J = 7.8 Hz, 1H), 8.153-8.167 (m, 3H), 8.22 (s, 1H) ppm. FAB-MS (*m/z*): [M+] calcd. For $C_{45}H_{43}N_3O_4S$: 721.3: found 722.3 [M+1].

2.2.2 Synthesis of SQ2

130 mg (0.19 mmol) *tert*-butyl ester of unsymmetrical squaraine dye (9) was dissolved in 3 mL of trifluoroacetic acid (TFA) and stirred for 3 h at room temperature. TFA was evaporated after completion of the hydrolysis which was monitored using TLC. The crude product was purified by silica gel chromatography using 10% methanol in ethyl acetate as eluent to give 65 mg of **SQ2** as blue solid (55%).^{1}H-NMR (400 MHz, CD_3OD, TMS): δ 1.5214-1.5563 (t, J = 14 Hz, 3H), 1.89 (s, 3H), 4.4928-4.5152 (q, J = 9 Hz, 2H), 5.4850 (s, 1H), 6.5698 (s, 1H), 7.3271-7.3651 (m, 2H), 7.4742-7.5108 (m, 2H), 7.678-7.6991 (d, J = 8.4 Hz, 2H), 7.7492-7.7707 (d, J = 8.6 Hz, 1H), 8.0011-8.0113 (d, J = 4.1 Hz, 1H), 8.1034-8.1632 (m, 3H), 8.2001-8.2225 (d, J = 9 Hz, 2H) ppm. FAB-MS (*m/z*): [M+] calcd. For $C_{37}H_{27}N_3O_4S$: 609.17: found 610.17 [M+1].

2.3 Fabrication and Characterization of DSSC

The fluorine doped tin oxide (FTO) purchased from Pilkington (TEC-8, 8Ω/sq) were prepared for TiO_2 working electrode by stepwise cleaning procedure using distilled water and finally using a mixture of acetone, ethanol and isopropanol (1:1:1) by intense sonication. Then it was subjected to UV-O_3 treatment for 20 min. The TiO_2 blocking layer was spin-coated on an FTO substrate at 2000 r.p.m. using 0.15 M titanium diisopropoxidebis(acetylacetonate) solution (75 wt% in isopropanol) in 1-butanol. The photoanodes were coated by

TiO_2 paste having particle size of 20 nm using doctor-blade method and then annealed at 500 °C for 30 min. TiO_2 scattering paste consisting larger rutile TiO_2 particles (0.5 μm, G2) was coated on top of the first layer and annealed at 150 °C for 15 min. This was immersed in 0.04 M aqueous $TiCl_4$ solution at 70 °C for 30 min. The electrodes were then put into programmed heating furnace at 500 °C for 30 min and then slowly cooled down to room temperature. The TiO_2 electrodes were immersed into squaraine dye solutions in ethanol (0.1 mmol) containing CDCA (20 mmol) and kept at room temperature for 15 h. Counter electrodes were prepared by thermal decomposition at 450 °C by dropping H_2PtCl_6 solution (7 mM in isopropanol) on FTO plates having pre-drilled holes and cleaned using the same procedure as for photoanodes. The dye adsorbed TiO_2 working electrodes and Pt counter electrodes were assembled with hot press using 60 μm surlyn spacer. The space in between both the electrodes were filled with liquid I^-/I_3^-electrolyte which was composed of various compositions of 1-ethyl-3-methylimidazolium iodide (EMII) or 1-propy-3-methylimidazolium iodide (PMII), lithium iodide (LiI), I_2 in ACN. The drilled holes were sealed with microscopic cover slide and surlyn to avoid electrolyte leakage.

Photocurrent−voltage (J-V) measurements were performed using a Keithly model 2400 source measure unit. The solar simulator (yamasita) equipped with a 1000 W Xenon lamp was used as a light source. The light intensity was adjusted with an NREL calibrated Si solar cell with KG-5 filter. A black aperture mask was attached on the cells during the measurements. Incident photon-to-current conversion efficiency (IPCE) was measured as a function of wavelength ranging from 300 to 800 nm using a specially designed IPCE system for DSSCs (PV measurements, Inc.). A 75 W Xenon lamp was used as a light source for generating monochromatic beam.

3. Results and discussion

3.1 Design and synthesis

In order to gain better understanding on the role of molecular geometry in determining the sensitizing efficiency of squaraine dyes, we have designed two structurally differed unsymmetrical squaraines. A cynaoacylic acid anchoring group was incorporated on the aromatic indolium moiety to get efficient dye adsorption on the TiO_2 surface and to improve the electron injection from the lowest unoccupied molecular orbital (LUMO) of dyes to the conduction band (CB) of TiO_2. In our best knowledge, there are only few reports on unsymmetrical squaraines that possess cynaoacylic acid anchoring group directly linked to the indolium acceptor part [28,29]. The introduction of an indole unit into the squaraine molecular frame work as the acceptor unit can effectively lead to red-shift in the absorption spectra compared to other commonly used acceptors, which is eventually beneficial for DSSC applications. The bulky *tert*-butyl group present on the SQ1 recognized to suppress the aggregation of sensitizer on TiO_2 and also helps to increase the solubility in common organic solvents. Therefore, this study certainly leads to a more extensive knowledge regarding the influence of structural modification on the efficiency of DSSCs.

3.2 Photophysical properties

The electronic absorption spectra of SQ1 and SQ2 measured in DCM showed intense absorption of these dyes in the visible to NIR region attributed to intramolecular charge transfer characteristics of squaraines and extended π–electron conjugation. In DCM, SQ1 and SQ2 showed absorption maxima at 630 and 613 nm respectively, which were assigned to the highest occupied molecular orbital (HOMO) to LUMO electronic transition. In these maximum wavelengths, the molar extinction (ε) value of SQ1 (7.56×10^4 M^{-1} cm^{-1}) was slightly higher than that of SQ2 (5.52×10^4 M^{-1} cm^{-1}). Both dyes showed a hypsochromic shift in wavelength maxima with increasing solvent polarity indicating a more polar nature for the ground state of the dye compared to the excited state. The red-shift in the absorption maximum of SQ1 in comparison to SQ2 might be due to the presence of electron donating *tert*-butyl groups on the peripheral carbazole donor, which stabilizes the LUMO of squaraine dye thereby reducing the energy gap. As expected, the emission maxima of SQ1 get red-shifted compared to that of SQ2 in different solvents. The dyes exhibited fluorescence emission at 692 and 680 nm in tetrahydrofuran (THF) and at 702 and 692 nm in DCM for SQ1 and SQ2 respectively.

The absorption spectra of both dyes on TiO_2 electrodes are much broader than that of solution state and which indicates the increased interaction of the dyes on the TiO_2 surfaces. Donor-acceptor molecules linked via π–conjugated linkers are prone to form aggregates due to their tendency to undergo strong dipole–dipole and π–π stacking interactions between the monomeric units. Squaraines are well known for their aggregate formation in solution as well as in solid state and such aggregates of sensitizing dyes can influence the photosensitizing efficiencies through expanding the absorption coverage [19, 30-32]. Thus, adsorption studies of both dyes on TiO_2 surface were performed in the absence and presence of co-adsorbent CDCA. It is well known that CDCA act as a de-aggregation agent through competitive adsorption on the semiconductor surface [22, 33]. It was found that adsorption behaviour of SQ1 get improved while that of SQ2 get limited with increasing concentration of CDCA in the dye soaking solution. Normalized absorption of both dyes in the different CDCA concentration showed identical nature, indicative of the same adsorbed species in all the experimental conditions.

3.3 Electrochemical properties

In order to use a dye as sensitizer for DSSCs, electron transfer from the excited dye to the CB of TiO_2 occurs efficiently and for these LUMO energy level of the dye should be higher in energy than the CB of TiO_2 (-0.5 V*vs.* NHE). At the same time, HOMO energy level of the dye should be lower in energy than that of the I^-/I_3^-redox electrolyte (0.40 V *vs.* NHE) for rapid dye regeneration from the resulting oxidized dye. The oxidation potential of SQ1 and SQ2 were measured via cyclic voltammetry (CV) and square wave voltammetry to understand their HOMO energy levels. The measurements were carried out with 1×10^{-3} M of the dyes in DCM at a scan rate of 100 mVs^{-1} using Ag/AgCl reference electrode that was calibrated using ferrocene.

The ground state oxidation potentials E_{ox} which correspond to the HOMO levels were 1.21 and 1.27 V respectively for SQ1 and SQ2 (Table 1). The calculated $E_{0\text{-}0}$ values are 1.85 and 1.87 eV for SQ1 and SQ2 respectively. The LUMO value calculated are -0.64 and -0.6 V *vs.* NHE for both the dyes respectively. The LUMO levels were only slightly more negative than CB edge of TiO_2 (-0.5 V *vs.* NHE) and this leads to a diminished driving force for electron injection from the LUMO of dyes to CB of TiO_2. This energy values revealed that the structural difference did not affected greatly on the HOMO and LUMO levels of both dyes.

Table 1: Photophysical and electrochemical characteristics of SQ1 and SQ2.

	$E_{0\text{-}0}$ (eV)	E_{ox}[a]/E_{red} *vs.* NHE (V)	HOMO[b]/LUMO[c] (eV)	HOMO/LUMO[d] (eV)
SQ1	1.85	1.21/-0.64	-5.25/-3.4	-5.35/-3.42
SQ2	1.87	1.27/-0.6	-5.31/-3.44	-5.46/-3.49

[a] Potentials measured *vs.* Ag/AgCl were converted to NHE by considering Fc/Fc^+ as +0.76 V *vs.* NHE in DCM; [b] HOMO = -[(E_{ox} *vs.* Fc/Fc^+) + 4.80]; [c] LUMO = HOMO + $E_{0\text{-}0}$; [d] HOMO and LUMO calculated by theoretical modeling.

3.4 Theoretical calculations

DFT was performed at the B3LYP/6-311G (d,p) level using Gaussian 09 program to optimize the molecular geometries and hence the frontier molecular orbitals (FMOs) of SQ1 and SQ2. From the optimized geometries of the dyes and the dihedral angles between the carbazole and thiophene parts, it can be noted that the carbazole moiety is twisted by 46-51° towards upper and 42-46° towards bottom with respect to the plane of thiophene ring while the rest of the π–conjugated portion of the dyes are coplanar (Figure 1). This suggests that both SQ1 and SQ2 possess almost similar geometric features and the carbazole moiety is mainly responsible for maintaining an overall non-planar geometry of these molecules. This non-planar geometry might help to prevent close π–π aggregation between the monomer units on the semiconductor surfaces. Also, the decreased interaction between the molecules enhances the thermal stability of the dyes.

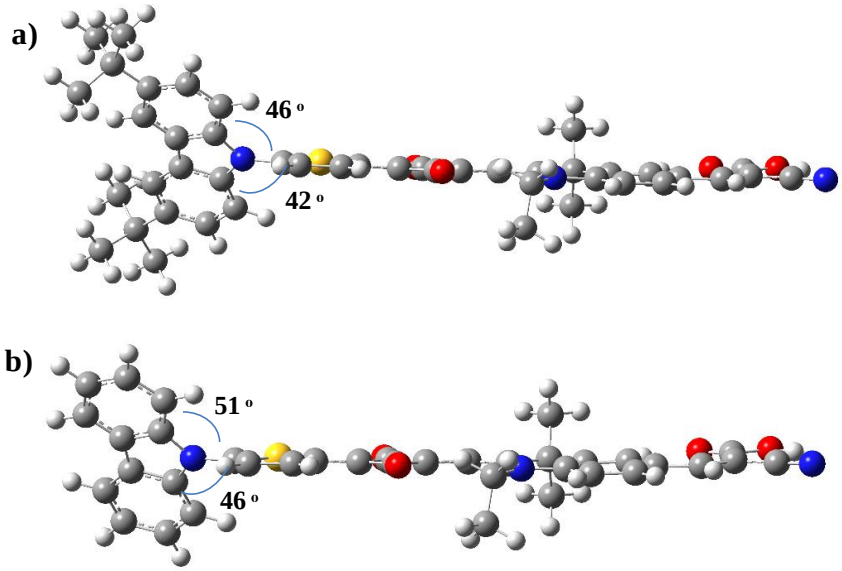

Figure 1: Optimized geometries of SQ1 (a) and SQ2 (b) using M06/6-31G (d,p) DFT method with dihedral angle between thiophene and carbazole parts.

3.5 Solar cell performance

The J-V characteristics measured under the illumination of AM 1.5 G simulated sunlight (100 mW/cm^2) are depicted in Figure 2 and the photovoltaic parameters are illustrated in Table 2.

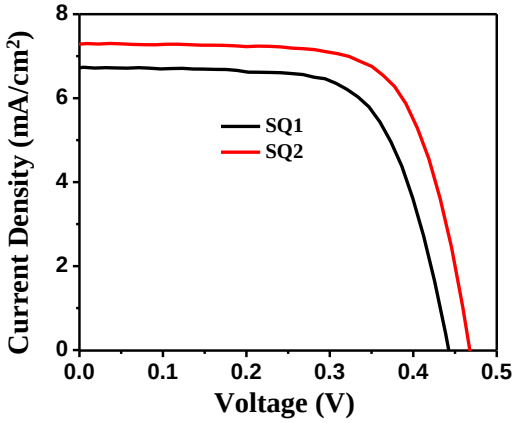

Figure 2: Current density–voltage characteristics for DSSCs from the device based on SQ1 and SQ2 under illumination of simulated sunlight (AM 1.5, 100 mW/cm^2).

The device performances of both dyes indicate that DSSCs with SQ2 sensitizer shows slightly improved overall conversion efficiency (η) of 2.38% with a short-circuit current density (J_{sc}) value of 7.28 mA/cm^2, open-circuit voltage (V_{oc}) of 0.46 V and fill factor (FF) of 69.8% over SQ1 sensitizer in the optimized condition having I^-/I_3^- as redox electrolyte. The electrolyte combination used was 0.6 M EMII with 0.03 M I_2 and 0.05 M LiI in ACN. Additives such as guanidinium thiocyanate and 4-tert-butylpyridine were not included in the electrolytes. Under the similar experimental conditions, SQ1 based device yielded an overall efficiency of 2.01% with a Jsc of 6.72 mA/cm^2, Voc of 0.44 V and FF of 67.69%. The thickness of TiO_2 film used for DSSCs was 16 µm (12 µm nanoparticle layer with 4 µm scattering layer).

Table 2: Photovoltaic performances of the DSSCs with devices based on SQ1 and SQ2 under illumination of simulated sunlight (AM 1.5, 100 mW/cm^2).

Dye	J_{sc} [mA/cm^2]	V_{oc} [V]	FF [%]	η [%]
SQ1	6.72	0.44	67.69	2.01
SQ2	7.28	0.46	69.8	2.38

Use of other electrolyte combination like PMII instead of EMII didn't show any further improvement in the device efficiency. Both dyes possess closely lying LUMO energy levels with respect to the CB of TiO_2 and it greatly affected the electron injection capability. Li salts are added usually along with liquid electrolyte because lithium cation can promote efficient electron injection through downward shifting of the conduction band edge of TiO_2 [34]. Thus, influences of lithium cation on the photovoltaic performance were studied and it was found that addition of increasing amount of LiI on to the electrolyte composition lead to deterioration of the device performance.

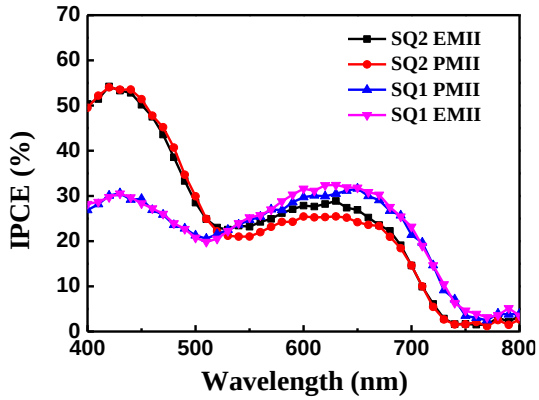

Figure 3: IPCE curves for DSSCs based on SQ1 and SQ2. The electrolyte used was 0.6 M EMII and PMII along with 0.03 M I_2 and 0.05 M LiI.

The evaluation of the IPCE spectra of cells based on SQ1 and SQ2 is displayed in Figure 3. As seen from the Figure, the IPCE spectra cover the visible region in the range of 400-750 nm, which facilitate efficient conversion of solar energy to electricity in DSSCs. The new peak observed in the IPCE curve might be due to the H-aggregate formation on the TiO_2 surfaces [19,35]. SQ1 possess slightly higher contribution in the longer wavelength region attributed to monomer band than that of H-aggregate, whereas SQ2 have a significantly higher contribution from the H-aggregate than that of monomer band. The increased contribution observed from the H-aggregate state of SQ2 than that to SQ1 may be associated with their structural difference. Absence of bulky tertiary butyl groups on the carbazole backbone of SQ2 facilitates easy H-aggregate formation on the semiconductor surfaces. The results clearly suggest that photoinjection and charge separation occurs in an improved way from the H-aggregates of SQ2 than its monomers.

From the photovoltaic parameters displayed in Table 2, it is evident that SQ1 and SQ2 have nearly same photovoltaic parameters. The slightly higher FF and J_{sc} value exhibited by SQ2 sensitized device is mainly accountable for its increased efficiency compared to that of SQ1 sensitized device. The most significant difference between these two dyes is related to the bulkiness of the end groups. However, the structural difference of the dyes could not lead to significant difference in their solar cell performances. The position of LUMO of both dyes much close to the TiO_2 CB limits the electron injection ability. The increased acceptor strength due to the presence of strong electron accepting cynoacrylic anchoring groups in both SQ1 and SQ2 results the shift of LUMO downwards compared to their parent squaraines [35]. However, the broad absorption coverage of SQ2 due to the H-aggregates on the semiconductor surface contributed to the improved performance than that of SQ1. Our study clearly demonstrates that unsymmetrical squaraine dyes with requisite energy levels having strong tendency to form H-aggregated state can lead to enhancement in DSSC performance by facilitating efficient panchromatic sensitization of the nanocrystalline TiO_2 electrode.

4. Conclusions

The donor-acceptor unsymmetrical squaraine dyes (SQ1 and SQ2) synthesized were employed as sensitizers in dye-sensitized solar cells. These dyes differed only with respect to the bulky tert-butyl groups present on the carbazole backbone. The highest occupied molecular orbital (HOMO) energy level of both dyes well located for efficient regeneration using I^-/I_3^- redox electrolytes, whereas the lowest unoccupied molecular orbital (LUMO) energy levels were positioned at potential much close to the conduction band of TiO_2 resulting in lack of enough driving force for electron injection. Theoretical calculations were performed to optimize the molecular geometries and hence the electron density distribution of SQ1 and SQ2. Much close LUMO energy level of both dyes with respect to conduction band edge of TiO_2 affected the Jsc value considerably. However, the IPCE spectra displayed significantly higher contribution in the higher energy region due to H-aggregates. Under optimized condition SQ1 and SQ2 showed an efficiency of 2.01 and 2.38% respectively. As evident from the IPCE spectrum, the improvement in the efficiency of SQ2 could be partly attributed to enhanced contribution from the H-aggregated state.

Authors' contributions

All authors contributed equally to the conception, design, experimental work, data analysis, interpretation of results, and preparation of the manuscript. All authors reviewed and approved the final version of the manuscript for publication.

Conflicts of interest

The author declares no conflict of interest.

Funding

This research received no external funding.

Data availability

No new data were created.

References

[1] B. O'Regan, M. Grätzel, A low-cost, high-efficiency solar cell based on dye-sensitized colloidal TiO_2 films, *Nature* **353** (1991) 737–740.

[2] M.K. Nazeeruddin, F. D. Angelis, S. Fantacci, A. Selloni, G. Viscardi, P. Liska, S. Ito, T. Bessho, M. Grätzel, Combined experimental and DFT-TDDFT computational study of photoelectrochemical cell ruthenium sensitizers, *J. Am. Chem. Soc*. **127** (2005) 16835–16847.
[3] Y. Cao, Y. Bai, Q. Yu, Y. Cheng, S. Liu, D. Shi, F. Gao, P. Wang, Dye-sensitized solar cells with a high absorptivity ruthenium sensitizer featuring a long alkyl chain, *J. Phys. Chem. C* **113** (2009) 6290–6297.
[4] G. Li, K.-J. Jiang, Y.-F. Li, S.-L. Li, L.-M. Yang, Efficient dye-sensitized solar cells based on triphenylamine dyes, *J. Phys. Chem. C* **112** (2008) 11591–11599.
[5] Y. Ooyama, Y. Harima, Molecular designs and syntheses of organic dyes for dye-sensitized solar cells, *Eur. J. Org. Chem*. (2009) 2903–2934.
[6] A. Mishra, M.K.R. Fischer, P. Bäuerle, Metal-free organic dyes for dye-sensitized solar cells: from structure-property relationships to design rules, *Angew. Chem. Int. Ed*. **48** (2009) 2474–2499.
[7] M.-W. Lee, J.-P. Kim, D.-H. Lee, M.J. Ko, Organic dyes containing fluorene moieties for efficient dye-sensitized solar cells, *ACS Appl. Mater. Interfaces* **6** (2014) 4102–4110.
[8] W. Zeng, Y. Cao, Y. Bai, Y. Wang, Y. Shi, M. Zhang, F. Wang, C. Pan, P. Wang, Efficient dye-sensitized solar cells with an organic sensitizer featuring orderly conjugated ethylenedioxythiophene and dithienosilole blocks, *Chem. Mater*. **22** (2010) 1915–1925.
[9] S. Sreejith, P. Carol, P. Chithra, A. Ajayaghosh, A simple donor-acceptor dye for efficient dye-sensitized solar cells, *J. Mater. Chem*. **18** (2008) 264–274.
[10] H. Choi, P.K. Santra, P.V. Kamat, Light-harvesting and charge-transfer properties of CdSe quantum dot sensitized solar cells, *ACS Nano* **6** (2012) 5718–5726.
[11] C. Qin, W.-Y. Wong, L. Han, Organic sensitizers for dye-sensitized solar cells: recent advances and perspectives, *Chem. Asian J*. **8** (2013) 1706–1719.
[12] T. Maeda, S. Arikawa, H. Nakao, S. Yagi, H. Nakazumi, Novel metal-free organic dyes containing heteroaromatic units for dye-sensitized solar cells, *New J. Chem*. **37** (2013) 701–708.
[13] J.-Q. Jiang, C.-L. Sun, Z.-F. Shi, H.-L. Zhang, Organic dyes with enhanced electron transport properties for dye-sensitized solar cells, *RSC Adv*. **4** (2014) 32987–32996.
[14] L. Beverina, R. Ruffo, M.M. Salamone, E. Ronchi, M. Binda, D. Natali, M. Sampietro, Organic π-conjugated dyes for efficient dye-sensitized solar cells, *J. Mater. Chem*. **22** (2012) 6704–6713.
[15] H. Sasabe, T. Igrashi, Y. Sasaki, G. Chen, Z. Hong, J. Kido, High-performance donor-acceptor organic dyes for dye-sensitized solar cells, *RSC Adv*. **4** (2014) 42804–42810.
[16] J.W. Ryan, T. Kirchartz, A. Viterisi, J. Nelson, E. Palomares, Understanding the role of recombination in dye-sensitized solar cells, *J. Phys. Chem. C* **117** (2013) 19866–19874.
[17] H. Choi, P.V. Kamat, Quantum dot solar cells: progress, challenges, and opportunities, *J. Phys. Chem. Lett*. **4** (2013) 3983–3991.
[18] S.P. Singh, G.D. Sharma, Recent developments in organic sensitizers for dye-sensitized solar cells, *Chem. Rec*. **14** (2014) 419–435.
[19] S. Alex, U. Santhosh, S. Das, Photophysical studies of donor-acceptor dyes for solar energy conversion, *J. Photochem. Photobiol. A* **172** (2005) 63–70.
[20] J.H. Yum, P. Walter, S. Huber, D. Rentsch, T. Geiger, F. Nuësch, F.D. Angelis, M. Grätzel, M.K. Nazeeruddin, Efficient far red sensitization of nanocrystalline TiO_2 films by an unsymmetrical squaraine dye, *J. Am. Chem. Soc*. **129** (2007) 10320–10321.
[21] S.S. Pandey, R. Watanabe, N. Fujikawa, G.M. Shivashimpi, Y. Ogomi, Y. Yamaguchi, S. Hayase, Synthesis and photovoltaic properties of organic dyes for dye-sensitized solar cells, *Tetrahedron* **69** (2013) 2633–2640.
[22] Y. Shi, R.B.M. Hill, J.H. Yum, A. Dualeh, S. Barlow, S.R. Marder, M. Grätzel, M.K. Nazeeruddin, High-performance organic sensitizers containing fluorene moieties for dye-sensitized solar cells, *Angew. Chem. Int. Ed*. **50** (2011) 6619–6623.
[23] F.M. Jradi, X. Kang, D. O'Neil, G. Pajares, Y.A. Getmanenko, P. Szymanski, T.C. Parker, M.A. El-Sayed, S.R. Marder, Near-infrared organic sensitizers for solar energy conversion, *Chem. Mater*. **27** (2015) 2480–2488.
[24] T. Jadhav, R. Misra, S. Biswas, G.D. Sharma, Donor-π-acceptor organic dyes for efficient dye-sensitized solar cells, *Phys. Chem. Chem. Phys*. **17** (2015) 26580–26588.
[25] K. Brunner, A.V. Dijken, H. Börner, J.J.A.M. Bastiaansen, N.M.M. Kiggen, B.M.W. Langeveld, White organic light-emitting devices for solid-state lighting, *J. Am. Chem. Soc*. **126** (2004) 6035–6042.
[26] T. Sudyoadsuk, S. Pansay, S. Morada, R. Rattanawan, S. Namuangruk, T. Kaewin, S. Jungsuttiwong, V. Promarak, Triphenylamine-based organic sensitizers for dye-sensitized solar cells, *Eur. J. Org. Chem*. (2013) 5051–5063.
[27] K. Gräf, M.K.A. Rahim, S. Das, M. Thelakkat, Efficient metal-free organic dyes containing thiophene units for dye-sensitized solar cells, *Dyes Pigm*. **99** (2013) 1101–1107.
[28] G.M. Shivashimpi, S.S. Pandey, R. Watanabe, N. Fujikawa, Y. Ogomi, Y. Yamaguchi, S. Hayase, Novel donor-acceptor dyes for dye-sensitized solar cells, *Tetrahedron Lett*. **53** (2012) 5437–5440.
[29] G.M. Shivashimpi, S.S. Pandey, R. Watanabe, N. Fujikawa, Y. Ogomi, Y. Yamaguchi, S. Hayase, Photophysical and photovoltaic studies of donor-acceptor dyes for dye-sensitized solar cells, *J. Photochem. Photobiol. A* **273** (2014) 1–7.
[30] G.D. Miguel, M. Ziołek, M. Zitnan, J.A. Organero, S.S. Pandey, S. Hayase, A. Douhal, Excited-state dynamics in dye-sensitized solar cells investigated by ultrafast spectroscopy, *J. Phys. Chem. C* **116** (2012) 9379–9389.
[31] G. Chen, H. Sasabe, W. Lu, X.F. Wang, J. Kido, Z. Hong, Y. Yang, Highly efficient organic sensitizers for dye-sensitized solar cells, *J. Mater. Chem. C* **1** (2013) 6547–6554.
[32] K.C. Deing, U. Mayerhöffer, F. Würthner, K. Meerholz, Organic semiconductor materials for photovoltaic applications, *Phys. Chem. Chem. Phys*. **14** (2012) 8328–8336.
[33] S. Ito, H. Miura, S. Uchida, M. Takata, K. Sumioka, P. Liska, P. Comte, P. Péchy, M. Grätzel, High-conversion-efficiency organic dye-sensitized solar cells, *Chem. Commun*. (2008) 5194–5196.
[34] S. Soman, M.A. Rahim, S. Lingamoorthy, C.H. Suresh, S. Das, Molecular engineering of organic sensitizers for dye-sensitized solar cells, *Phys. Chem. Chem. Phys*. **17** (2015) 23095–23104.
[35] C. Li, W. Wang, X. Wang, B. Zhang, Y. Cao, Novel organic sensitizers containing thiophene derivatives for dye-sensitized solar cells, *Chem. Lett*. **34** (2005) 554–555.